Optics Letters

Extended eigenvalue calibration method for Mueller matrix polarimetry with four photoelastic modulators

Wenlong Chen,[1] Xiuguo Chen,[1,2,*] Yifu Wang,[1] Shilong Yang,[1] Hang Yue,[1] Jing Hu,[1] and Shiyuan Liu[1,2]

[1]State Key Laboratory of Intelligent Manufacturing Equipment and Technology, Huazhong University of Science and Technology, Wuhan 430074, China
[2]Optics Valley Laboratory, Wuhan 430074, China
*xiuguochen@hust.edu.cn

Received 18 October 2024; revised 2 January 2025; accepted 2 January 2025; posted 3 January 2025; published 22 January 2025

The Mueller matrix polarimeter with four photoelastic modulator (4-PEM MMP), known for its high-speed and high-precision measurement capabilities, holds great potential in material characterization and nanoscale measurements. We propose an extended eigenvalue calibration method (eECM) to the 4-PEM MMP by introducing two temporal basis vectors to project the continuously modulated light intensity into a time-independent projection matrix, which can then be acquired by a nonlinear regression method. The eECM enables complete calibration of system parameters of the 4-PEM MMP in a model-free manner without any approximation, including the parameters associated with each PEM and the alignment errors in the azimuths of all the polarization elements. Moreover, it is unnecessary to precisely adjust the orientations of the polarization elements, and it does not require precise reference sample information either. Consequently, the eECM allows the 4-PEM MMP to achieve accurate Mueller matrix measurement under not only the usual system configurations but also other unusual system configurations in a simple and unified approach. Simulation results have verified the effectiveness and advantages of the eECM.

https://doi.org/10.1364/OL.545387

Photoelastic modulator (PEM) is an optical element widely used for precise manipulation of light polarization [1–4]. Retardance is a crucial parameter for the PEM, with its specific formula shown below:

$$\delta(t) = F\sin(2\pi vt + \varphi) + \delta_0, \tag{1}$$

where F is the amplitude controlled by the voltage, v is the frequency, φ is the initial phase at $t = 0$, and δ_0 is the static retardation. By precisely controlling the retardance, researchers can effectively manipulate the polarization states of light for optical characterization of complex samples and observation of biological tissues [5–7]. The Mueller matrix polarimeter with four PEMs (4-PEM MMP) allows for the fast and simultaneous measurement of the complete 4×4 Mueller matrix without any moving elements and demonstrates a great potential in material characterization [8].

As illustrated in Fig. 1, a 4-PEM MMP typically consists of a polarizer and two PEMs in the polarization state generator (PSG) and another two PEMs and an analyzer in the polarization state analyzer (PSA). The azimuths of the polarization elements, including the azimuths of the transmission axes of the polarizer and analyzer θ_{P} and θ_{A} and the azimuths of the fast axes of the four PEMs θ_{1-4}, are fixed in actual measurements, whose combination is referred to as the system configuration. To simply data analysis, the azimuths of the polarization elements are usually chosen to be 0°, ±45°, or ±90°, which we referred to as the usual system configurations, since the sample Mueller matrix elements can be expressed individually using the coefficients of the trigonometric functions of the PEM's retardance or their products under the above usual configurations [8]. Otherwise, the deduction procedure of the Mueller matrix elements becomes quite complicated.

To realize accurate Mueller matrix measurement, delicate system calibration needs to be performed for the 4-PEM MMP. Current methods primarily calibrate the parameters F and δ_0 of each PEM as well as the alignment errors in the azimuths of the polarization elements, by establishing a system model for the usual configuration [8–10]. Moreover, many approximations need to be made to reduce model complexity during the calibration. For example, the influence of higher frequency components in the detected signal is ignored. Static retardations and alignment errors are assumed to be quite small to allow for the first-order Taylor approximation. The calibrated alignment errors are then used to guide adjustment of the orientations of the polarization elements with precise rotation stages. In addition, it necessitates limiting the bandwidth of the detected signal to prevent spectral leakage in data analysis. Recently, Arteaga *et al.* proposed a pseudo-inverse method (PIM) using the complete temporal basis of PEM modulation for measuring the Mueller matrix elements in the 4-PEM MMP [11], circumventing the spectral leakage issue.

As opposed to the above model-based methods, the eigenvalue calibration method (ECM) is a model-free method, which is traditionally developed for discrete time-domain polarization modulation systems, such as MMPs based on liquid crystals

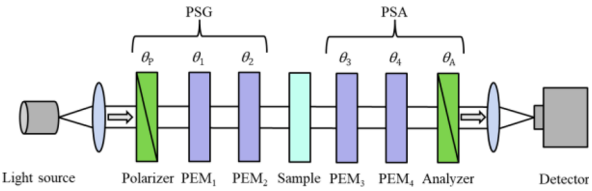

Fig. 1. Schematic diagram of the 4-PEM MMP. PSG, polarization state generator; PSA, polarization state analyzer; θ_P and θ_A, azimuths of the polarizer and analyzer; θ_k ($k = 1, 2, 3, 4$), azimuths of the PEM$_k$.

[12–15]. The ECM only requires the measurement of a series of reference samples, such as air, polarizers, and wave plates, and transforms the calibration procedure into an eigenvalue problem of a system of linear equations [16,17]. Later, we applied the ECM to a dual rotating-compensator MMP (DRC-MMP) by introducing two basis vectors and projecting the continuously modulated light intensity into a projection matrix, extending the ECM to the continuous time-domain polarization modulation systems [18]. Although the 4-PEM MMP is also a continuous time-domain polarization modulation system, the unique modulation principle of the PEM makes the design of the basis vectors to extend the ECM for the 4-PEM MMP differ significantly from that of the DRC-MMP.

In this Letter, we propose an extended ECM (eECM) for the 4-PEM MMP to achieve system calibration. A major contribution is the introduction of two temporal basis vectors, which project the continuously modulated light intensity into a time-independent projection matrix. The projection matrix is then acquired by a nonlinear regression method. The eECM enables a complete calibration of the 4-PEM MMP parameters in a model-free manner, including (F, φ, δ_0) associated with each PEM and the alignment errors in the azimuths of all polarization elements, without any approximation. Similar to PIM, the eECM circumvents spectral leakage by utilizing the complete temporal basis of PEM modulation. Since the azimuth information are inherently incorporated into the projection matrix, no further adjustments to the polarization element orientations are needed. Consequently, the eECM enables the 4-PEM MMP not only to the usual system configurations but also to other unusual system configurations in a unified approach.

Method. According to Fig. 1, the light intensity signal $I_{\text{out}}(t)$ collected by the detector in the 4-PEM MMP system is expressed as follows:

$$\begin{aligned} I_{\text{out}}(t) &= \begin{bmatrix} 1 & 0 & 0 & 0 \end{bmatrix} \cdot \mathbf{M}_{\text{PSA}}(t) \cdot \mathbf{M}_{\text{S}} \cdot \mathbf{M}_{\text{PSG}}(t) \cdot \boldsymbol{S}_{\text{in}} \\ &\equiv \boldsymbol{S}_{\text{PSA}}^{T}(t) \cdot \mathbf{M}_{\text{S}} \cdot \boldsymbol{S}_{\text{PSG}}(t), \end{aligned} \tag{2}$$

where $\boldsymbol{S}_{\text{in}} = [I_{\text{in}}, 0, 0, 0]^T$ is the Stokes vector of the incident light with I_{in} being the incident intensity, $\mathbf{M}_{\text{PSG}}$ and $\mathbf{M}_{\text{PSA}}$ are respectively the Mueller matrices of PSG and PSA, and $\mathbf{M}_{\text{S}}$ is the sample Mueller matrix. The detailed expressions of $\boldsymbol{S}_{\text{PSG}}(t)$ and $\boldsymbol{S}_{\text{PSA}}(t)$ are presented in Section 1 of Supplement 1. Generally, the system parameters in the 4-PEM MMP that need to be calibrated include the intrinsic parameters $\{F, \varphi, \delta_0\}$ of each PEM and the azimuths $\{\theta_P, \theta_1, \theta_2, \theta_3, \theta_4, \theta_A\}$ of all polarization elements., and v of each PEM can be obtained in real time through its own reference signal. For convenience, we divide the above system parameters into two categories according to their characteristics. One category is the dynamic system parameters including $\{F, \varphi\}$ of each PEM, since these parameters may fluctuate in each measurement due to the environmental disturbance and unstable control in operation [11]. Another category is the static system parameters including δ_0 of each PEM and $\{\theta_P, \theta_1, \theta_2, \theta_3, \theta_4, \theta_A\}$, since the former depend primarily on the quality and geometry of the PEMs, while the latter are determined by the initial installation, and they are unchanged in each measurement.

To achieve complete system calibration of the 4-PEM MMP, we introduce the basis vectors $\boldsymbol{\Theta}_{\text{W}}(t)$ for the PSG and $\boldsymbol{\Theta}_{\text{A}}(t)$ for the PSA as follows:

$$\boldsymbol{\Theta}_{\text{W}}(t) = \begin{bmatrix} 1, \sin(\hat{\delta}_1(t)), \sin(\hat{\delta}_2(t)), \\ \cos(\hat{\delta}_1(t)), \cos(\hat{\delta}_2(t)), \\ \sin(\hat{\delta}_1(t)) \sin(\hat{\delta}_2(t)), \\ \sin(\hat{\delta}_1(t)) \cos(\hat{\delta}_2(t)), \\ \cos(\hat{\delta}_1(t)) \cos(\hat{\delta}_2(t)), \\ \sin(\hat{\delta}_2(t)) \cos(\hat{\delta}_1(t)) \end{bmatrix}^T, \tag{3}$$

$$\boldsymbol{\Theta}_{\text{A}}(t) = \begin{bmatrix} 1, \sin(\hat{\delta}_4(t)), \sin(\hat{\delta}_3(t)), \\ \cos(\hat{\delta}_4(t)), \cos(\hat{\delta}_3(t)), \\ \sin(\hat{\delta}_4(t)) \sin(\hat{\delta}_3(t)), \\ \sin(\hat{\delta}_4(t)) \cos(\hat{\delta}_3(t)), \\ \cos(\hat{\delta}_4(t)) \cos(\hat{\delta}_3(t)), \\ \sin(\hat{\delta}_3(t)) \cos(\hat{\delta}_4(t)) \end{bmatrix}^T, \tag{4}$$

where $\hat{\delta}(t) = F \sin(2\pi v t + \varphi)$. Note that all the dynamic system parameters are included in the above two basis vectors. Projecting $\boldsymbol{S}_{\text{PSG}}$ and $\boldsymbol{S}_{\text{PSA}}$ onto the above basis vectors, respectively, Eq. (2) can be rewritten as follows:

$$\begin{aligned} I_{\text{out}}(t) &= I_{\text{in}}/4 \cdot \{\boldsymbol{\Theta}_{\text{A}}^{T}(t) \cdot \mathbf{A} \cdot \mathbf{M}_{\text{S}} \cdot \mathbf{W} \cdot \boldsymbol{\Theta}_{\text{W}}(t)\} \\ &= I_{\text{in}}/4 \cdot \{\boldsymbol{\Theta}_{\text{A}}^{T}(t) \cdot \mathbf{D} \cdot \boldsymbol{\Theta}_{\text{W}}(t)\}, \end{aligned} \tag{5}$$

where $\mathbf{W}$ and $\mathbf{A}$ are called the modulation matrix and analysis matrix, respectively, which are the projection matrices of $\boldsymbol{S}_{\text{PSG}}(t)$ and $\boldsymbol{S}_{\text{PSA}}(t)$ onto $\boldsymbol{\Theta}_{\text{W}}(t)$ and $\boldsymbol{\Theta}_{\text{A}}(t)$. The detailed expressions of $\mathbf{W}$ and $\mathbf{A}$ are presented in Section 1 of Supplement 1. Note that all the static system parameters are included into the matrices $\mathbf{W}$ and $\mathbf{A}$. The matrix $\mathbf{D} = \mathbf{A} \cdot \mathbf{M}_{\text{S}} \cdot \mathbf{W}$ is named the intensity projection matrix, which can be further used for the traditional ECM operation.

According to Eqs. (3)–(5), we can observe that the dynamic and static system parameters that need to be calibrated in the 4-PEM MMP are separated by the basis vectors $\boldsymbol{\Theta}_{\text{W}}(t)$ and $\boldsymbol{\Theta}_{\text{A}}(t)$. On the other hand, since the basis vectors $\boldsymbol{\Theta}_{\text{W}}(t)$ and $\boldsymbol{\Theta}_{\text{A}}(t)$ also include system parameters to be calibrated, the retrieval of the projection matrix $\mathbf{D}$ in the 4-PEM MMP differs significantly from that in the ECM for the DRC-MMP [18]. In this work, we propose a nonlinear regression method to acquire the projection matrix $\mathbf{D}$ while simultaneously calibrating the dynamic parameters in the basis vectors as follows:

$$\arg\min_{\boldsymbol{P}} ||\boldsymbol{I}_{\text{out}}^{\text{Exp}} - \boldsymbol{I}_{\text{out}}^{\text{Mod}}(\boldsymbol{P})||_2^2, \tag{6}$$

where the vector $\boldsymbol{P} = [D_{ij}, F_k, \varphi_k]$ consists of the parameters to be calibrated, with D_{ij} being the elements of the project matrix $\mathbf{D}$ ($i, j = 1, 2 \ldots, 9$), F_k, and φ_k being the dynamic system parameters of PEM$_k$ ($k = 1, 2, 3, 4$), $I_{\text{out}}^{\text{Exp}}$ denotes the measured intensity, and $I_{\text{out}}^{\text{Mod}} = \boldsymbol{\Theta}_{\text{A}}^{\text{T}}(t) \cdot \mathbf{D} \cdot \boldsymbol{\Theta}_{\text{W}}(t)$ is the calculated intensity according to Eqs. (3)–(5). Note that suitable initial values of $\boldsymbol{P}$ are necessary to ensure the convergence of Eq. (6), which actually can be easily obtained. The parameter F_k has an approximately linear relationship with the control voltage, allowing its

initial value close to the true value to be obtained by adjusting the control voltage. The initial value of φ_k can be extracted from the PEM reference signal, with its accuracy limited by the sampling frequency, and it is very close to the true value. The initial value of the projection matrix **D** can be randomly generated as a 9×9 matrix, since it serves as the projection of light intensity onto the two basis vectors with each element considered as the coefficient of a series of basis vectors. Since the basis vectors are linearly independent, there is no correlation between the elements. Therefore, although there are many parameters to be calibrated, the only and accurate parameters can still be achieved, allowing the model to accurately fit the data.

The aim of the subsequent calibration is to obtain the modulation matrix **W** and the analysis matrix **A**, which include static system parameters to be calibrated, i.e., the azimuth information of all the polarization elements and the static retardation of each PEM The solution of **A** and **W** follows the traditional ECM, with details provided in Section 2 of Supplement 1. Note that the 4-PEM MMP is an overdetermined system, and here **A** is a 9×4 matrix and **W** is a 4×9 matrix. To obtain accurate eigenvalues and reduce the impact of noise, an optimal 4×4 submatrix is extracted from the projection matrix **D** for eigenvalue calculation by minimizing the condition number of the submatrix [13]. Note that since the static retardation of each PEM is generally small, the second row of **A** and the second column of **W** are typically close to zero. Thus, the second row and second column of the projection matrix **D** should be avoided when choosing the 4×4 submatrix. Note that the above calibration procedure is described for any wavelength. For spectroscopic measurement, the above calibration can be performed in a wavelength-by-wavelength manner.

Results and discussion. To examine the validity of eECM for the 4-PEM MMP, we conducted a series of simulations under a usual system configuration [11], where the azimuths of the polarizer and analyzer were 45° and −45° and the azimuths of the four PEMs were 90°, 45°, 45°, and 90°, respectively. The modulation amplitudes of the four PEMs were $F_1 = 2.85$ rad, $F_2 = 3.53$ rad, $F_3 = 4.22$ rad, and $F_4 = 2.64$ rad, and these values are randomly selected within a reasonable range. The φ of the four PEMs were 1.6581 rad, and the PEM frequencies were $\nu_1 = 42{,}066$ Hz, $\nu_2 = 49{,}787$ Hz, $\nu_3 = 59{,}721$ Hz, and $\nu_4 = 47{,}077$ Hz. Based on the above usual configuration, using the azimuth of the polarizer as the reference, the azimuth errors of the four PEMs and the analyzer were set as 0.4°, −0.7°, 0.2°, −0.5°, and 0.4°, respectively. Additionally, the static retardation values of the four PEMs were set to be 0.004 rad, 0.008 rad, 0.006 rad, and 0.005 rad, respectively [8]. To further make the simulation more realistic, a Gaussian random noise of about 27 dB was added to the intensity signal $I_{\text{out}}(t)$ calculated by Eq. (2), which is in accordance with the stability and noise level of a real system's light source and detector [19]. In all simulations, the sampling rate and the number of sampling points were set as 4×10^6 Hz and $N = 5\times10^4$. The reference samples during the calibration were air, a polarizer, and a 1/4 wave plate, which are in accordance with the traditional ECM in [12].

The acquisition of the projection matrix **D** is the prerequisite of the successful implementation of the eECM. To examine the feasibility of the acquisition of **D** via the nonlinear regression method described in Eq. (6), simulations were carried out for the selected reference samples. As can be observed from Fig. 2, the reconstructed intensity $I_{\text{out}}^{\text{Mod}}$ exhibits excellent agreement with the "measured" intensity $I_{\text{out}}^{\text{Exp}}$ (ground truth in Fig. 2). Here, the

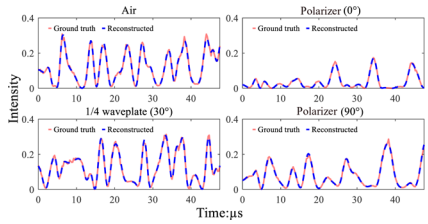

Fig. 2. Nonlinear fitting results of different reference samples, including air, polarizer (0°), 1/4 wave plate (30°), and polarizer (90°). Here, the degrees appended to the reference samples are their azimuths.

"measured" intensity $I_{\text{out}}^{\text{Exp}}$ was synthesized according to Eq. (2) added with 27 dB Gaussian noise. The calibration errors of the parameters $\boldsymbol{P}$ are presented in Section 3 of Supplement 1. During the regression, the initial values of D_{ij} ($i, j = 1, 2, \ldots, 9$) were random values between 0 and 1, and the initial values of F_k and φ_k ($k = 1, 2, 3, 4$) had offsets of 0.5 rad, and 0.1 rad, respectively, to their preset values in the simulation. The results presented in Fig. 2, as well as in Fig. S1 and Tables S1 and S2 in Supplement 1, clearly demonstrate the feasibility of the proposed nonlinear regression in the acquisition of the projection matrix **D** and the dynamic system parameters F and φ of each PEM.

With the acquired projection matrix **D**, we can further obtain the modulation matrix **W** and the analysis matrix **A** via the eECM, which contain the static system parameters to be calibrated, i.e., the azimuths of polarization elements and the static retardation of each PEM. Note that **W** and **A** can be directly used in the measurement of samples without the need for further adjusting the orientations of the polarization elements according to the calibrated results. To validate the feasibility of the direct use of the calibrated **W** and **A** in measurement, a polarizer and a 1/3 wave plate were selected as the samples under test (SUT) [20]. Note the difference between the SUT and the reference samples during the calibration. Actually, there are no specific requirements for the SUT here. The SUT were examined at different azimuths from 0° to 180°, with a 10° interval. As shown in Fig. 3, the "measured" Mueller matrices of simulation show excellent agreement with the theoretical values. Here, the "measured" sample Mueller matrices were obtained by $\mathbf{M}_{\text{SUT}} = \mathbf{A}^{+}\mathbf{D}\mathbf{W}^{+}$, and the superscript "+" denotes the Moore–Penrose pseudo-inverse. The results thus demonstrate the feasibility of eECM in the calibration of the static system parameters and direct measurement of the Mueller matrices of samples.

One of the distinctive advantages of the proposed eECM is that it allows the 4-PEM MMP to achieve accurate Mueller matrix measurement under not only the usual system configurations but also other unusual system configurations. To validate this, we designed three different system configurations, named as C1, C2, and C3. The azimuths $\{\theta_{\text{P}}, \theta_1, \theta_2, \theta_3, \theta_4, \theta_{\text{A}}\}$ of the polarization elements under the three system configurations were set as follows: C1 = {45°, 90°, 45°, 45°, 90°, −45°}, C2 = {0°, 30°, 60°, 65°, 30°,50°}, and C3 = {0°, 10°, 50°, 100°, 140°,95°}, respectively. Note that here C1 belongs to the usual system configuration. A polarizer and a 1/3 wave plate were selected as the SUT, which were examined at different azimuths from 0° to 180°, with a 10° interval.

Figure 4 presents the Mueller matrix errors $\Delta\mathbf{M}$ between the "measured" sample Mueller matrices via the eECM and their

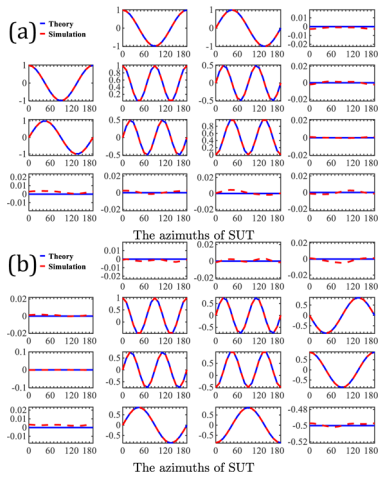

Fig. 3. Comparison of Mueller matrices for samples under test (SUT) at different azimuths in the simulation. (a) Polarizer and (b) 1/3 wave plate.

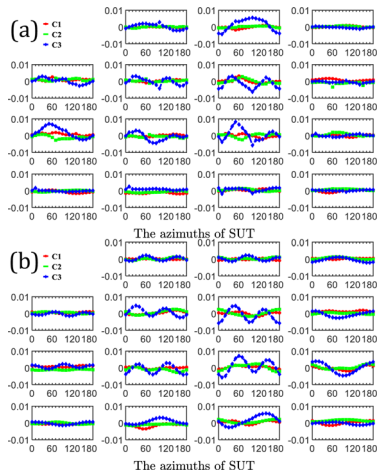

Fig. 4. Mueller matrix errors $\Delta\mathbf{M}$ for samples under test (SUT) at multiple azimuths achieved under three system configurations C1, C2, and C3. (a) Polarizer and (b) 1/3 wave plate.

theoretical values at different sample azimuths. The calibrated errors of **A** and **W** associated with different system configurations are presented in Section 4 of Supplement 1. As can be observed, the measurement errors of all Mueller matrix elements under the three configurations for both the wave plate and polarizer are within 0.007, with the errors of some elements being below 0.002. Here, the Mueller matrix errors are primarily attributed to the random noise in the synthetic intensities. Multiple averages would be expected to further reduce the errors. Consequently, we have verified that our proposed eECM enables the 4-PEM MMP not only to the usual system configurations but also to other unusual system configurations in a simple and unified approach.

Conclusion. In conclusion, we have extended the ECM to the 4-PEM MMP. The proposed eECM can achieve complete calibration of system parameters of the 4-PEM MMP in a model-free manner without any approximation. The eECM allows the 4-PEM MMP to achieve accurate Mueller matrix measurement under not only the usual system configurations but also other unusual system configurations. For multi-PEM systems, this method is simpler and easier to implement compared to traditional methods, and it does not require precise reference sample information, offering a new perspective for calibrating multi-PEM systems.

Funding. National Natural Science Foundation of China (62175075, 52022034, 52130504); Interdisciplinary Research Program of Huazhong University of Science and Technology (2023JCYJ047); Innovation Project of Optics Valley Laboratory (OVL2023PY003).

Disclosures. The authors declare no conflicts of interest.

Data availability. Data underlying the results presented in this Letter are not publicly available at this time but may be obtained from the authors upon reasonable request.

Supplemental document. See Supplement 1 for supporting content.

REFERENCES

1. K. W. Hipps and G. A. Crosby, J. Phys. Chem. **83**, 555 (1979).
2. G. E. Jellison and F. A. Modine, Appl. Opt. **36**, 8190 (1997).
3. W. Guan, G. A. Jones, Y. Liu, *et al.*, J. Appl. Phys. **103**, 043104 (2008).
4. A. Gribble, D. Layden, and I. A. Vitkin, Opt. Lett. **38**, 5272 (2013).
5. O. Arteaga and B. Kahr, J. Opt. Soc. Am. B **36**, F72 (2019).
6. S. Alali, A. Gribble, and I. Alex Vitkin, Opt. Lett. **41**, 1038 (2016).
7. O. Arteaga and B. Kahr, Opt. Lett. **38**, 1134 (2013).
8. O. Arteaga, J. Freudenthal, B. Wang, *et al.*, Appl. Opt. **51**, 6805 (2012).
9. W. Quan, Q. Wang, Y. Zhai, *et al.*, Appl. Opt. **56**, 4491 (2017).
10. J. Kurtz, A. S. Alenin, and J. S. Tyo, Appl. Opt. **62**, 1635 (2023).
11. J. Gomis-Brescó and O. Arteaga, Opt. Lett. **48**, 1966 (2023).
12. E. Compain, S. Poirier, and B. Drevillon, Appl. Opt. **38**, 3490 (1999).
13. P. A. Letnes, I. S. Nerbø, L. M. S. Aas, *et al.*, Opt. Express **18**, 23095 (2010).
14. C. Macías-Romero and P. Török, J. Eur. Opt. Soc.-Rapid Publ **7**, 12004 (2012).
15. Y. Yu, N. Baba-Ali, and G. M. Gallatin, PhotoniX **1**, 18 (2020).
16. L. M. S. Aas, P. G. Ellingsen, B. E. Fladmark, *et al.*, Opt. Express **21**, 8753 (2013).
17. S. A. Rosales, E. Garcia Caurel, and R. Ossikovski, Opt. Lett. **49**, 1165 (2024).
18. S. Sheng, X. Chen, C. Chen, *et al.*, Opt. Lett. **46**, 4618 (2021).
19. F. Goudail, Opt. Lett. **42**, 2153 (2017).
20. P. Li, D. Lv, H. He, *et al.*, Opt. Express **26**, 3791 (2018).